DRAFT VERSION JANUARY 6, 2016
Preprint typeset using LaTeX style emulateapj v. 5/2/11

A COMPACT X-RAY SOURCE IN THE RADIO PULSAR-WIND NEBULA G141.2+5.0

STEPHEN P. REYNOLDS[1] & KAZIMIERZ J. BORKOWSKI[1]

Draft version January 6, 2016

ABSTRACT

We report the results of a 50 ks *Chandra* observation of the recently discovered radio object G141.2+5.0, presumed to be a pulsar-wind nebula. We find a moderately bright unresolved X-ray source which we designate CXOU J033712.8 615302 coincident with the central peak radio emission. An absorbed power-law fit to the 241 counts describes the data well, with absorbing column $N_H = 6.7(4.0, 9.7) \times 10^{21}$ cm^{-2} and photon index $\Gamma = 1.8(1.4, 2.2)$. For a distance of 4 kpc, the unabsorbed luminosity between 0.5 and 8 keV is $1.7^{+0.4}_{-0.3} \times 10^{32}$ erg s^{-1} (90% confidence intervals). Both L_X and Γ are quite typical of pulsars in PWNe. No extended emission is seen; we estimate a conservative 3σ upper limit to the surface brightness of any X-ray PWN near the point source to be 3×10^{-17} erg cm^{-2} s^{-1} arcsec^{-2} between 0.5 and 8 keV, assuming the same spectrum as the point source; for a nebula of diameter $13'$, the flux limit is 6% of the flux of the point source. The steep radio spectrum of the PWN ($\alpha \sim -0.7$), if continued to the X-ray without a break, predicts L_X (nebula) $\sim 1 \times 10^{33}$ erg s^{-1}, so additional spectral steepening between radio and X-rays is required, as is true of all known PWNe. The high Galactic latitude gives a z-distance of 350 pc above the Galactic plane, quite unusual for a Population I object.

Subject headings: ISM: individual objects (G141.2+5.0) — ISM: jets and outflows — pulsars: general

1. INTRODUCTION

Pulsar-wind nebulae, the bubbles of relativistic particles and magnetic field blown by pulsars, perform several important astrophysical functions. Most simply, they can serve as calorimeters for the energy loss from pulsars, allowing the inference of unseen pulsars beamed away from us. But they also serve as laboratories for the study of the behavior of highly relativistic flows at shock waves, so are useful in the study of extragalactic jets and gamma-ray burst sources. Pulsar-wind nebulae (PWNe) were originally defined by radio properties: center-filled morphology, flat radio spectrum ($\alpha \sim -0.3 - 0$, with $S_\nu \propto \nu^\alpha$) and (relatively) high polarization – properties originally found in only a handful of objects (an early catalog, Weiler 1985, lists eight "pure" PWNe and another five "well-established" PWNe inside radio shells). However, the launch of *Chandra*, and to a lesser extent *XMM-Newton,* ushered in a new era in the discovery of pulsars and PWNe. Finally, the advent of TeV and GeV studies, primarily with H.E.S.S., MAGIC, and VERITAS at TeV energies, and Fermi and Agile in GeV, has revealed a trove of hard-spectrum, center-brightened sources, many of which turn out to harbor pulsars, and (almost) all of which are therefore presumed to be PWNe – many at a much older age than previous objects, old enough to have long outlived their natal supernova remnant (SNR) shell. Kargaltsev, Rangelov, & Pavlov (2013) list 76 pulsars containing X-ray and/or TeV PWNe. See Gaensler & Slane (2006) for a general review of PWNe.

There are now enough PWNe known that general properties of the class are fairly well understood – or at least have become familiar. The initial pulsar wind seems to be "dark," that is, cold in the fluid frame and radiating inefficiently. The wind is thermalized in some fashion in a termination shock marking the inner edge of the observed PWN (Rees & Gunn 1974), where the characteristic bright synchrotron emission (ranging from radio to X-ray wavelengths) appears. Particles are transported downstream into the nebula by some combination of advection and diffusion, until the outer edge of the PWN where the wind interacts either with the interior of a more-or-less "normal" shell SNR, or, if it is much older, with undisturbed ISM. However, none of those processes is well understood.

The wind leaving the pulsar is almost certainly dominated by Poynting flux, but probably needs to be particle-dominated at the termination shock, to allow there to be a shock at all (Kennel & Coroniti 1984a). The ratio of magnetic to particle energy flux, the "magnetization" σ, apparently must drop by orders of magnitude in the dark zone. However, the spherical Kennel & Coroniti (1984a) hydrodynamic model does not take account of the "striped wind" feature of an oblique rotating neutron star, in which the azimuthal magnetic field beyond the light cylinder changes direction with the pulsar's rotation. Thus magnetic reconnection is highly likely, and will affect the magnetization in the dark zone. Additionally, it is likely that the magnetization at the termination shock is a function of latitude. These effects can be seen in recent 3D MHD simulations (Porth et al. 2013), in which solutions exist with varying σ and significantly higher average values.

At the shock, the outgoing kinetic energy is somehow turned into random particle energy. The spectrum of particles released into the nebula, as inferred from the synchrotron spectral-energy distribution (SED), appears initially quite flat ($N(E) \propto E^{-s}$ with $s \equiv 1 - 2\alpha \sim 1 - 2$ for radio-emitting particles), but all PWNe show steepening at higher photon energies. The extent to which this is due to intrinsic physics of the thermalization instead of post-shock evolutionary effects is not known. The initial particle acceleration is probably not traditional diffusive shock acceleration, since the shock is both relativistic and probably almost exactly perpendicular, as the wind is expected to contain a very tightly wound Parker spiral of magnetic field. Particle acceleration by magnetic reconnection is an attractive possibility, but quantitative predictions are difficult. In any case, the detailed nature of the particle energization process remains obscure.

[1] Department of Physics, North Carolina State University, Raleigh, NC 27695-8202; reynolds@ncsu.edu

One major problem in understanding particle energization at PWN shocks concerns the relation of radio emission to that at higher energies. Kennel & Coroniti (1984b) simply threw up their hands at the problem of the Crab Nebula's radio emission, as it could not easily be accommodated in their otherwise very successful scheme of an ideal steady MHD outflow in spherical geometry. Suggested solutions typically invoke a totally separate particle population produced through a separate process; e.g., Atoyan (1999), who proposes that the radio-emitting electrons were injected early in the life of the nebula and have simply aged since. (This picture requires the Crab pulsar to have been born with an initial rotation period of 3 – 5 ms, a striking assertion.) Additionally, steepening of the spectrum between radio and X-rays by an amount greater than the increase in power-law index of 0.5 expected for synchrotron losses in homogeneous sources is almost universally observed (e.g., data in Chevalier 2005). Is this an intrinsic property of the particle acceleration mechanism? If so, in the wind, at the termination shock, or elsewhere? Advection models can reproduce this steepening purely from evolutionary effects on an initial straight power-law (Reynolds 2009) at the expense of invoking ad-hoc gradients in source properties. The comparison of X-ray and radio properties is the most effective way to address these important questions; ideally, X-ray observations can also reveal the powering neutron star, even if it is not detectable in radio pulsations.

2. G141.2+5.0

The discovery of additional PWNe has occurred in recent years primarily at very high photon energies. However, those objects have turned out mostly to be far older and interacting directly with ISM, introducing additional complications in modeling. An alternative approach is to start with objects of known radio properties, the original defining characteristics of PWNe. One such object, only recently discovered, is G141.2+5.0, found in Canadian Galactic Plane Survey (CGPS; Taylor et al. 2003) observations using the Dominion Radio Astronomy Observatory (DRAO) at 1.4 GHz (Kothes et al. 2014, hereafter K14). This object, the first radio-discovered PWN in 17 years (see Fig. 1), has a 1.4 GHz flux density of 0.14 Jy, and center-brightened morphology with high radio polarization (15% integrated over the source, but reaching 40% at peak). It thus has all the earmarks of a normal radio PWN – except for the spectrum, which is much steeper: $\alpha = -0.69 \pm 0.05$, more characteristic of an extragalactic source (even a little too steep for typical shell SNRs). K14 review alternate possible interpretations of the source, but the complete absence of obvious counterparts in infrared, optical, or soft X-ray surveys rules out H II regions or nearby radio galaxies. Cluster halos normally have too steep spectra ($\alpha \lesssim -1.0$) while cluster relics have similarly steep spectra but also much less spherical morphologies. The discovery we report here of an X-ray point source coincident with the intensity peak of G141.2+5.0 essentially confirms the PWN interpretation.

G141.2+5.0 shows the center-brightened morphology and substantial (also center-brightened) linear polarization characteristic of the class. H I observations give a kinematic distance of 4 ± 0.5 kpc, but also reveal a surrounding shell of H I with a radius of about $6'$, expanding at 6 km s^{-1} (K14). Faraday rotation observations imply a substantial amount of internal Faraday rotation, indicating significant thermal ionized gas. These latter properties, along with the steep radio spectrum, make G141.2+5.0 a highly unusual PWN.

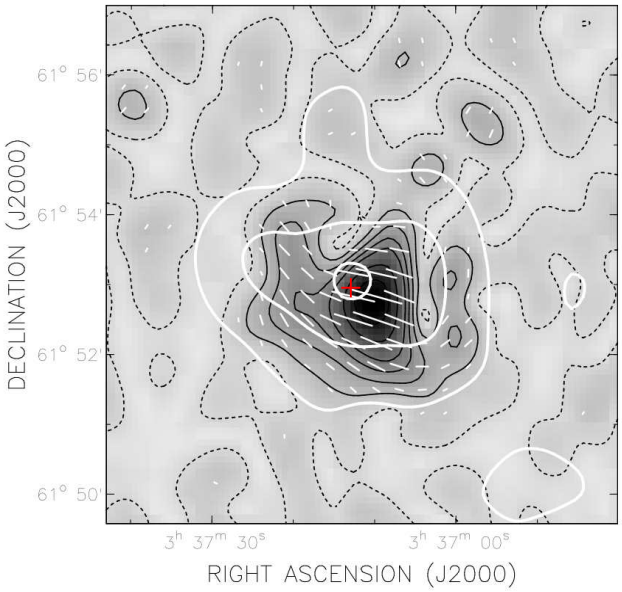

Figure 1. DRAO image in polarized intensity at 1420 MHz of G141.2+5.0 (Kothes et al. 2014). The resolution is $56'' \times 48''$. Total-intensity contours are shown in white. The bulge in the lowest contour is an unrelated point source The point-source position is indicated by the red cross (much larger than the positional uncertainty).

While the radio spectrum of G141.2+5.0 is anomalous for a PWN, K14 cite two other PWNe with steep radio spectra: G76.9+1.0 (Landecker et al. 1993) and DA 495 (Kothes et al. 2008). G76.9+1.0 shows a fairly circular envelope of diameter about $7'$ enclosing two maxima in radio (Fig. 2; Landecker et al. 1993), and a known pulsar between them: with a period of 24 ms and a rotational energy-loss $\dot{E} = 1.2 \times 10^{38}$ erg s^{-1}, it is the second most energetic pulsar in the Galaxy (Arzoumanian et al. 2011). (This confirms that unprepossessing nebulae may contain unusual pulsars.) It also contains a tiny ($16'' \times 10''$) X-ray nebula, shown as the faint contours near the center in Fig. 2. The small size and low flux of its X-ray PWN may be typical for PWNe with steep radio spectra; J2022+3842 has a very low efficiency η of turning spindown power into PWN X-ray luminosity: $L_X(\mathrm{PWN}) \sim 6 \times 10^{32}$ erg s^{-1} for a distance of 10 kpc (Arzoumanian et al. 2011), and $\eta \sim 2 \times 10^{-5}$. (Its magnetospheric efficiency is about 10 times larger, that is, $L_X(\mathrm{PWN}) \sim 0.1 L_X(\mathrm{pulsar})$). DA 495, with a radio extent of about $20'$, also has a very small X-ray nebula (about $40''$), with a central point source thought to be a pulsar, though pulsations have not been detected (Karpova et al. 2015).

3. OBSERVATIONS AND ANALYSIS

We observed G141.2+5.0 with *Chandra* for 17.5 ks on 16 November 2014, and for 32 ks on 28 November 2014 (obsIDs 16758 and 17551, respectively), with the ACIS S3 CCD chip. All data were reprocessed with *CIAO* v4.7 and CALDB v4.6.8, and screened for periods of high particle background. The absence of bright X-ray sources from the ROSAT All-Sky Survey in the vicinity of G141.2+5.0 ensured that any emission would be of low surface brightness, so we used Very Faint mode for more efficient background rejection. Spectral analysis was done with XSPEC v12.8.2 (Arnaud 1996). Background was extracted from a large area on the S3 CCD

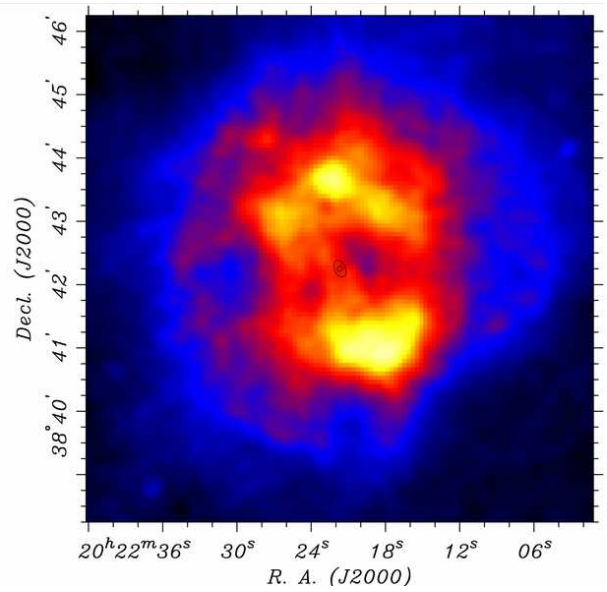

Figure 2. DRAO image in total intensity at 1420 MHz of G76.9+1.0 (Landecker et al. 1993). The resolution is $15'' \times 14''$. Contours near the center show the X-ray PWN (Arzoumanian et al. 2011).

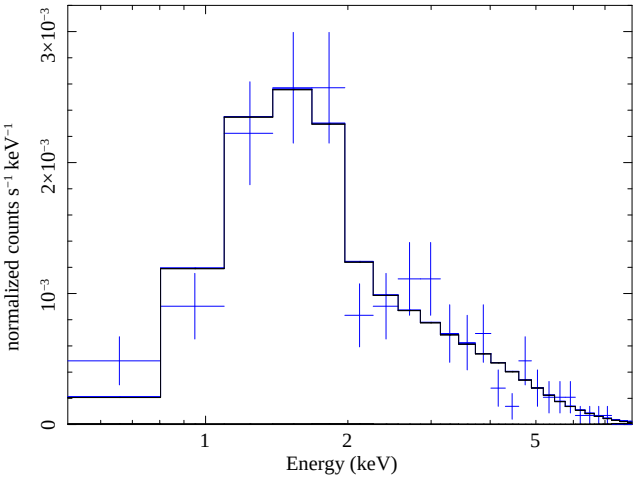

Figure 3. Spectrum of X-ray point source, with the best-fit power law model shown.

chip away from G141.2+5.0. The background was modeled instead of subtracted in order to allow the use of Markov chain Monte Carlo (MCMC) methods that is necessary for the unbiased estimation of spectral model parameters for faint X-ray sources (e.g., van Dyk et al. 2001). We assumed non-informative priors in spectral fits, either uniform or logarithmic, with the latter used only for (absorbed) fluxes. No spectral binning was used, expect when plotting spectra and model fits.

We detected a moderately bright source at the location (α, δ) = ($3^h37^m12.86^s$, $61°53'1.9''$), containing 241 counts, which we designate CXOU J033712.8 615302. These coordinates are the average of positions in individual pointings, $3^h37^m12.892^s$ ($3^h37^m12.824^s$) and $61°53'2.01''$ ($61°53'1.77''$) for observations 17551 (16758). They correspond to source centroids estimated with help of the `srcextent` tool in *CIAO*. The source size estimated with `srcextent` is consistent with an unresolved point source. The positional uncertainty is almost entirely due to the *Chandra* external astrometric errors (mean error of $0.''16$; Rots 2009). Statistical errors are significantly smaller, and equal to $0.''07$ ($0.''09$) for observations 17551 (16758). These errors were estimated from equation (14) of Kim et al. (2007). As there are no optical or radio counterparts to this X-ray source (or to other X-ray sources sufficiently close to the *Chandra* optical axis to allow for reliable measurements of their positions), a more accurate determination of the source position is currently not possible.

The source location is near the peak brightness of the radio image (Fig. 1). Three other much fainter point sources can be seen within the extent of the radio nebula. Each has about 20 cts; if they have the same spectral shape as G141.2+5.0, their fluxes are about 8×10^{-15} erg cm^{-2} s^{-1} (see below). At this level, the number of sources per square degree found in the *Chandra* Deep Field South is about 400 (Lehmer et al. 2012), or about 0.1 arcmin^{-2}. Since the radio extent of G141.2+5.0 is over 8 arcmin^{-2}, we can be reasonably sure these are unassociated background sources, probably AGNs which dominate the counts at this flux level (Lehmer et al. 2012).

With this number of counts, only simple spectral fitting was possible. We made MCMC fits with power-law and blackbody spectral distributions in the energy range from 0.5 keV to 8 keV (all detected source counts are within this energy range), allowing for absorption if necessary. The power-law and blackbody fits are equally acceptable, but the temperature of the blackbody ($0.93^{+0.10}_{-0.08}$ keV) is unreasonably high for a putative neutron star with no evidence of youth. Furthermore, no interstellar absorption is required for the best-fit blackbody (95% upper limit to N_H is 2.0×10^{21} cm^{-2}). There is significant extinction ($E(B-V) = 0.64^{+0.033}_{-0.035}$) within 1 kpc in this direction on the sky (Green et al. 2015), so the blackbody fit is inconsistent with the 4 kpc distance derived from the H I absorption measurements toward G141.2+5.0.

The power-law fit, shown in Figure 3, gives an absorbing column $N_H = 6.7(4.0, 9.7) \times 10^{21}$ cm^{-2} (using the Grevesse & Sauval [1998] abundance set), reasonable if the point source is at the 4 kpc distance of the radio PWN. The power-law index is $\Gamma = 1.8(1.4, 2.2)$, quite typical for X-ray pulsars (see, e.g., the catalog in Kargaltsev et al. 2013). The (absorbed) flux between 0.5 and 8 keV is $6.1(5.2, 7.1) \times 10^{-14}$ erg cm^{-2} s^{-1}. After calculating unabsorbed fluxes for each MCMC draw (i.e., a triple consisting of N_H, Γ, and the absorbed flux), we arrived at an unabsorbed flux of $9.0(7.6, 11.1) \times 10^{-14}$ erg cm^{-2} s^{-1}, giving an unabsorbed luminosity within this energy range of $L_X = 1.7(1.4, 2.1) \times 10^{32}$ erg s^{-1} at 4 kpc.

The timing analysis was performed on observations that were corrected to barycenter using the *CIAO* task `axbary` (with the source coordinates listed above). We searched for pulsations in photon arrival times in the frequency range from about $\nu_{min} = 0.08$ Hz to $\nu_{max} = 0.159$ Hz. The minimum frequency corresponds to a rotation period of 12.5 s. This is slower than the rotation period of all known isolated neutron stars, including magnetars. The 3.141 s time resolution of our observations sets the highest ($1/6.282$ s = 0.159 Hz) fre-

quency to be searched. It also restricts our search to purely sinusoidal signals. We used the well-known Rayleigh (Z_1^2) test instead of phase folding because of its higher sensitivity (e. g., see Leahy et al. 1983). The number of independent frequency searches is $3T(\nu_{max}-\nu_{min})$, where $T = 301^h$ is the total time elapsed between the beginning and end of *Chandra* observations of G141.2+5.0 (the factor of 3 accounts for oversampling in frequency for the Z_1^2-test; De Jager et al. 1989). The maximum Z_1^2 power found, $Z_{1,\rm max}^2 = 19.8$, is not statistically significant in view of the large number of frequencies searched. This $Z_{1,\rm max}^2$, in combination with the total number of counts in the source extraction region, corresponds to an upper limit of 0.54 for the pulsed fraction (at 95% confidence; for this estimate, we used the method of Brazier 1994).

There is no apparent extended emission near the point source. In an annulus with inner and outer radii of 2.5 pixels (1.23″) and 13 pixels (6.4″), respectively, there are 27 counts in the 0.5–8 keV energy range. We used the *CIAO* task `arfcorr` to generate simple synthetic PSFs at several photon energies which were then combined to make predictions for ratios of counts in this annulus relative to an aperture with radius equal to the inner radius of the annulus. The measured counts within this aperture plus background estimates far from the source served as input to a two-component model consisting of a uniform background and a PSF model for the point source. This model predicts 23 counts within this annulus, so there is no evidence for diffuse emission from a PWN. Based on this model and assuming the same spectral shape for the PWN and the point source, a 3σ upper limit to the (absorbed) 0.5-8 keV PWN surface brightness near the point source is 3×10^{-17} erg cm^{-2} s^{-1} arcsec^{-2}, or 6% of the measured flux from the point source when integrated over the annulus.

4. DISCUSSION

Our discovery of the X-ray point source in G141.2+5.0 essentially confirms its identification as a PWN, in the rare class of steep-radio-spectrum PWNe. These objects also share properties of a point source (pulsar in one case) near the geometric center of the radio nebula, and very small X-ray nebulae (or, in the case of G141.2+5.0, only an upper limit). The point sources in DA 495 and G76.9+1.0 differ considerably in properties: in the former, the point source does not show pulsations (pulsed fraction $\lesssim 40\%$; Karpova et al. 2015), but is well fit by thermal models: a blackbody with $kT \sim 215$ eV, or a magnetized neutron-star atmosphere model with $kT \sim 80-90$ eV. The upper limit to a power-law contribution is $L_X \lesssim 5\times10^{31}$ erg s^{-1}. In G76.9+1.0, the X-ray point source is observed to be a pulsar, with a nonthermal spectrum with $\Gamma = 1.0$ and $L_X(2-10\ \rm keV) = 7\times10^{33}$ erg s^{-1} (Arzoumanian et al. 2011). The point source in G141.2+5.0 more closely resembles the pulsar in G76.9+1.0, though much less luminous and with a slightly steeper spectrum.

All evidence is consistent with our point source being the pulsar powering the radio PWN. (A search for radio pulsations has been performed [D. Lorimer, PI] but nothing has been reported.) The adequacy of a power-law fit points to the emission we observe being primarily magnetospheric in nature. This suggests a short duty cycle and high pulsed fraction for the pulsar (e.g., Kargaltsev & Pavlov 2007). However, its properties are not unusual for X-ray rotation-powered pulsars, and give no hint to the nature of the very unusual radio PWN that surrounds it.

We see no trace of extended emission that could be a pulsar-wind nebula. For an assumed diameter of 13″ (about 1/20 the radio size), our 3σ upper limit on the luminosity is about 10^{31} erg s^{-1} (assuming the same spectrum as the pulsar), making any PWN that size fainter than all but 5 of the 59 PWNe catalogued in Kargaltsev & Pavlov (2010). The ratio of X-ray to radio flux S_X/S_r for PWNe varies over a wide range, with a typical value being about 10 (e.g., Gaensler & Slane 2006), but ranging to 100 or more (e.g., 600 for the PWN in G11.2–0.3; Tam et al. 2002, Kargaltsev et al. 2013). A small early collection of radio-selected PWNe has S_X/S_r ranging from 10 to 1000 and above (Reynolds & Chevalier 1984), while the steep-spectrum PWN DA 495 has $S_X/S_r \sim 15$. Roughly estimating the integrated radio flux S_r of G141.2+0.5 as νS_ν gives $S_r \sim 2\times10^{-15}$ erg cm^{-2} s^{-1}. Then $S_X \sim 10S_r$ would imply an X-ray flux of order 2×10^{-14} erg cm^{-2} s^{-1}, about 1/5 of the flux in the point source, and three times the upper limit we find for a presumed PWN diameter of 26″. Alternatively, an extrapolation of the radio flux of 120 mJy at 1.4 GHz to 1 keV (2.4×10^{17} Hz) with $\alpha = -0.69$ would imply a spectral flux of about 35 nJy there, or an integrated flux between 0.5 and 8 keV (with the same spectral index) of 3×10^{-13} erg cm^{-2} s^{-1}, or about 20 times the flux in our point source and far greater than any PWN flux. We infer that, as with all other known PWNe with radio to X-ray spectra, the spectrum must steepen, even from its already steep radio value. Whether this is due to radiative losses or intrinsic spectral structure cannot be determined at this time.

In both DA 495 and G76.9+1.0, the X-ray nebula is smaller than the radio nebula by large factors (about 30 in each case). The same ratio in G141.2+5.0 would mean an X-ray nebula with radius about 4″. We see no evidence for extended emission beyond the PSF. Any X-ray PWN could be either smaller than 1/30 of the radio size, or considerably fainter than 10 times the radio flux. Either possibility would make G141.2+5.0 a unique pulsar/PWN combination in the Galaxy, whose further study might provide important clues to the late-time PWN phenomenon.

This work was supported by NASA through the *Chandra* General Observer Program grant GO5-16055X. The scientific results reported in this article are based on observations made by the *Chandra* X-ray Observatory. This research has made use of software provided by the *Chandra* X-ray Center (CXC) in the applications packages *CIAO* and *ChIPS*.

REFERENCES

Arnaud, K. A. 1996, in Astronomical Data Analysis and Systems V, eds. G. Jacoby & J. Barnes, ASP Conf. Series, v.101, 17
Arzoumanian, Z., Gotthelf, E. V., Ransom, S. M., et al. 2011, ApJ, 739, 39
Atoyan, A.M. 1999, A&A, 346, L49
Brazier, K. T. S. 1994, MNRAS, 268, 709
Chevalier, R.A. 2005, ApJ, 619, 839
De Jager, O. C., Swanepoel, J. W. H., & Raubenheimer, B. C. 1989, A&A, 221, 180
Gaensler, B.M., & Slane, P.O. 2006, ARA&A, 44, 17
Green, G. M., Schlafly, E. F., Finkbeiner, D. P., et al. 2015, ApJ, 810:25
Grevesse, N., & Sauval, A.J. 1998, SSRv, 85, 161
Kargaltsev, O., & Pavlov, G.G. 2007, Ap&SS, 308, 287
Kargaltsev, O., & Pavlov, G.G. 2010, in AIP Conf.Proc. v.1248, X-ray Astronomy 2009: Present Status, Multi-wavelength Approach and Future Perspectives, ed. A. Comastri, L. Angelini, & M. Cappi (Melville, NY: AIP), 25.
Kargaltsev, O., Rangelov, B., & Pavlov, G.G. 2013, arXiv:1305.2552
Karpova, A., Zyuzin, D., Danilenko, A., & Shibanov, Yu. 2015, MNRAS, 453, 2241
Kennel, C.F., & Coroniti, F.V. 1984, ApJ, 283, 694
Kennel, C.F., & Coroniti, F.V. 1984, ApJ, 283, 710
Kim, M., Kim, D.-M., Wilkes, B. J., et al. 2007, ApJS, 169, 401

Kothes, R., Landecker, T. L., Reich, W., Safi-Harb, S., & Arzoumanian, Z. 2008, ApJ, 687, 516
Kothes, R., Sun, X.H., Reich, W., & Foster, T.J. 2014, ApJ, 784, L26
Landecker, T. L., Higgs, L. A., & Wendker, H. J. 1993, A&A, 276, 522
Leahy, D. A., Elsner, R. F., & Weisskopf, M. C. 1983, ApJ, 272, L256
Lehmer, B.D., Xue, Y.Q., Brandt, W.N., et al. 2012, ApJ, 752:46
Porth, O., Komissarov, S. S., & Keppens, R. 2013, MNRAS, 431, L48
Rees, M.J., & Gunn, J.E. 1974, MNRAS, 167, 1
Reynolds, S.P. 2009, ApJ, 703, 662
Reynolds, S.P., & Chevalier, R.A. 1984, ApJ, 278, 630
Rots, A. 2009, Determining the Astrometric Error in CSC Source Positions, http://cxc.harvard.edu/csc/memos/files/Rots_CSCAstrometricError.pdf
Tam, C., Roberts, M. S. E., & Kaspi, V. M. 2002, ApJ, 572, 202
Taylor, A.R., Gibson, S.J., Peracaula, M., Martin, P.G., Landecker, T.L., Brunt, C.M., Dewdney, P.E., Dougherty, S.M., Gray, A.D., Higgs, L.A., Kerton, C.R., Knee, L.B.G., Kothes, R., Purton, C.R., Uyaniker, B., Wallace, B.J., Willis, A.G., & Durand, D. 2003, AJ, 125, 3145
van Dyk, D. A., Connors, A., Kashyap, V. L., & Siemiginowska, A. 2001, ApJ, 548, 224
Weiler, K.W. 1985, in *The Crab Nebula and Related Supernova Remnants* (ed. Kafatos, M.C., & Henry, R.B.C.) (Cambridge: Cambridge U. Press), 265